Enhancement of large-scale flood damage assessments using building-material-based vulnerability curves for an object-based approach

Johanna Englhardt[1], Hans de Moel[1], Charles K. Huyck[2], Marleen C. de Ruiter[1], Jeroen C. J. H. Aerts[1], Philip J. Ward[1]

[1]Institute for Environmental Studies (IVM), Vrije Universiteit Amsterdam, De Boelelaan 1087, 1081HV Amsterdam, The Netherlands
[2]ImageCat Inc., Long Beach, CA 90802, USA

Correspondence to: Johanna Englhardt (j.englhardt@vu.nl)

Abstract. In this study, we developed an enhanced approach for large-scale flood damage and risk assessments that uses characteristics of buildings and the built environment as object-based information to represent exposure and vulnerability to flooding. Most current large-scale assessments use an aggregated land-use category to represent the exposure, treating all exposed elements the same. For large areas where previously only coarse information existed such as in Africa, more detailed exposure data is becoming available. For our approach, a direct relation between the construction type and building material of the exposed elements is used to develop vulnerability curves. We further present a method to differentiate flood risk in urban and rural areas based on characteristics of the built environment. We applied the model to Ethiopia, and found that rural flood risk accounts for about 22% of simulated damages; rural damages are generally neglected in the typical land-use-based damage models particularly at this scale. Our approach is particularly interesting for studies in areas where there is a large variation in construction types in the building stock, such as developing countries. It also enables comparison across different natural hazard types that also use material-based vulnerability, paving the way to the enhancement of multi-risk assessments.

1. Introduction

Globally, floods are one of the main natural hazards in terms of socioeconomic impacts, causing billions of dollars of damage each year. For example, between 1980 and 2013, global flood damages exceeded $1 trillion, and resulted in ca. 220,000 fatalities (Dottori et al., 2016). Reducing disaster risk, such as from flooding, is globally very high on the political agenda. For example, it is an important aspect of both the Sendai Framework for Disaster Risk Reduction (UNISDR, 2015) and the Warsaw International Mechanism for Loss and Damage Associated with Climate Change Impacts (UNFCCC, 2013). To achieve this reduction in risk at the global scale requires methods to quantitatively assess global flood risk (Mechler et al., 2014). Here, flood risk is defined as a function of three components: hazard (e.g. flood extent and depth), exposure (assets

and people exposed), and vulnerability (factors that determine the susceptibility of the exposed assets to the hazard) (UNISDR, 2015).

Global flood risk assessments are increasingly used in decision-making and practice, and have been useful for identifying flood risk hotspots (e.g. Ward et al., 2015). In an ideal situation, such flood risk assessment models could use detailed, high-resolution data for all locations around the globe (Jonkman, 2013). In practice, data and resources required for such models rarely exist, and therefore global flood risk models have been developed. Current global flood risk models often use resolutions between 30" x 30" and 0.5° x 0.5° to assess the exposed assets (e.g. Alfieri et al., 2013; Arnell and Gosling, 2016; Ward et al., 2013). Recently, much effort has been put into improving global risk models, mainly by improving the hazard component (e.g. Dottori et al., 2016; Ikeuchi et al., 2017; Sampson et al., 2015; e.g. Trigg et al., 2016). However, much less attention has been given to improvements in the representation of exposure and vulnerability, despite the fact that their overall contribution to uncertainty is large (de Moel and Aerts, 2010).

In large-scale assessments, i.e. regional to global levels, exposure is generally represented based on aggregated land-use categories, especially in regions where only limited data are available, such as Africa (de Moel et al., 2015). Whilst using such data provides a useful first assessment of large-scale damages and risk (e.g. Feyen et al., 2011; Hall et al., 2005; Ward et al., 2013), more detailed information of the exposed objects could improve these assessments. Vulnerability is mostly represented using stage-damage functions, also known as vulnerability curves, which describe the relationship between potential damages of the exposed elements for different levels of the hazard (usually water depth). For large-scale studies, a vulnerability curve is generally developed for each of the aggregated land-use categories used to represent exposure (Ward et al., 2013).

Whilst aggregated land-use categories may be a suitable option to represent exposure if data are limited, they cannot reflect the (spatial) heterogeneity within each land-use category (Wünsch et al., 2009). For instance, large-scale flood risk models usually focus on an 'urban' category that aggregates exposed elements of various types (e.g. houses, infrastructure, shops, green areas etc.) into one land-use class (Ward et al., 2015). Since an aggregated land-use category like 'urban' is coupled to one 'urban' vulnerability curve, these curves generalise the relationship between flood depth and damage across all of the diverse exposed element types within that category. Without a more direct relation between these types of exposed elements and the impact of flood waters, large uncertainties exist in the simulated damages (de Moel and Aerts, 2010). More detailed information on the specific land use, its extent, and the vulnerability of the exposed elements could improve large-scale assessments, for example by using high-resolution remote sensing products (Goldblatt et al., 2018; Myint et al., 2011) or information as used in local scale flood damages studies at an object level (individual buildings, businesses, infrastructure objects, etc.) (de Moel et al., 2015; Merz et al., 2010). In our approach, we therefor utilize information about the composition of an area's building stock and the characteristics of exposed objects, particularly construction types and materials. Applying these object-based information, which is not to be confused with object based image analysis in remote sensing, is contrasting to the common land-use-based approach in large scale flood risk assessments.

The literature distinguishes flood vulnerability of buildings according to different structural factors (such as building type, quality, height, and material), as well as occupancy type (such as residential, commercial, industrial, etc.). The latter is a commonly used factor for determining the vulnerability (de Ruiter et al., 2017), with much fewer studies relating potential losses to the structural factors. Reasons for this are the paucity of information and the huge effort it takes to obtain

5   information on the damage incurred by individual objects and the structural components (Wahab and Tiong, 2016). Studies or models that do include information on these factors are mostly based on surveys and were therefore only feasible on smaller scales. FLEMOps (Thieken et al., 2008) is an example of a model that uses survey data on flood damages in Germany, and includes factors such as building type and quality. The study by de Villiers et al. (2007) is one of the few assessments (see also World Bank, 2000) within Africa, but uses size and content value of houses to determine flood damage

10   and does not go into detail on structural features. Studies that focus on construction type and building material to assess the flood damage show that these characteristics, together with ground floor elevation and number of floors, are important features in determining the vulnerability of different building types to floods (e.g. Godfrey et al., 2015; Neubert et al., 2008; Schwarz and Maiwald, 2008; Zhai et al., 2005).

Compared to risk assessments in the earthquake domain where they are essential components (de Ruiter et al., 2017), or in

15   local-scale studies focusing on physical vulnerability to debris flows (Papathoma-Köhle et al., 2017), construction types and building materials have only played a minor role as indicators for flood vulnerability. Large-scale flood risk assessments could be improved by using object-based characteristics to represent exposure and vulnerability, particularly in developing countries with a diverse structural building stock.

Recently, a building exposure dataset has been developed for several African countries as part of the Building Disaster

20   Resilience program for the World Bank's Africa Disaster Risk Financing Initiative by ImageCat (ImageCat et al., 2017). ImageCat uses a stratified sampling technique that infers the number of buildings in a region from census data and then uses image processing tools to identify development patterns (Hu et al., 2014). The construction practices are then characterized through a review of the literature, interviews, review of VHR images, in situ video, and in some cases site visits (Silva et al., 2018). This characterization of development patterns is used for dasymetric mapping of building counts to a 15" grid.

25   Estimates are supplemented with total estimates of floor area, and replacement values based on construction practices observed in each development pattern (Huyck and Eguchi, 2017). Compared to the methods employed in current large-scale flood risk models, the information about the built environment of an area and its characteristics as provided in such datasets enables a differentiation between the exposed objects in terms of vulnerability to flood waters and exposed value.

Furthermore, a greater level of detail opens up the possibility to address the issue of distinguishing urban and rural flood risk.

30   This is commonly neglected in land-use-based flood risk assessment, due to the focus on higher value urban damages. Moreover, land-use classification studies have difficulties in assessing urban and rural differences. This is because the resolution in previous land-use and land-cover products was not sufficient to identify smaller settlements, and the characteristics of urban and rural areas are very different and can be difficult to grasp in land-use classification studies (Dijkstra and Poelman, 2014). Internationally there is no agreed way to distinguish urban from rural areas. For example,

according to the national census in Ethiopia, localities of 2,000 or more inhabitants are considered urban, whereas the urban definition for Niger only includes capitals of departments and districts (UNSD, 2016). Another traditional distinction is that urban areas provide a different way of life and usually a higher living standard (UNSD, 2017). Compared to developed countries, the building stock in rural areas of developing countries is often constructed from more traditional and less

5 expensive building materials, which makes them more vulnerable to flooding. In this regard, urban settlements in the context of this study are defined as geographic units with built-up area that are more developed and have a higher built-up density than rural settlements.

The aim of this paper is to develop an approach for assessing large-scale flood risk in urban and rural areas using object-based data from ImageCat to represent exposure, and to develop vulnerability curves for different building classes. The

10 approach draws upon common practices in earthquake risk assessments, and relates damage by flood waters more directly to the vulnerability of buildings based on the building materials. We test the suitability of this approach for the case of Ethiopia, comparing our results with those using a more traditional large-scale flood damage modelling approach, examining how the increased detail influences risk estimates.

2.   Data and Methods

15 The approach used in this study is composed of the following main four steps, and shown in Figure 1:

1) development of **vulnerability classes and curves** for different construction types and building materials based on a literature review of previous studies;

2) classification of an **object-based exposure** dataset using input data from ImageCat;

3) derivation of **maximum damage values** and

20 4) **risk assessment** by combining the aforementioned vulnerability and exposure with hazard data.

Each of these steps is described in more detail in the following subsections.
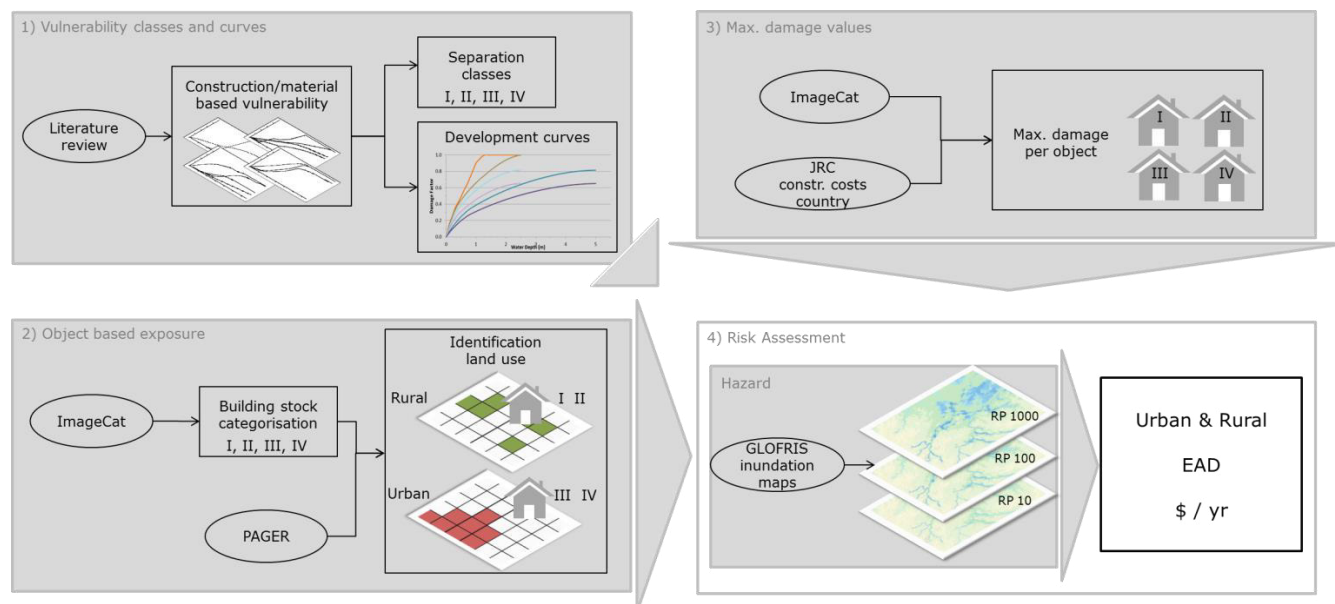
Figure 1 Flowchart for large-scale flood risk assessment using object-based data with a building-material-based vulnerability approach.

2.1. Vulnerability classes and curves

5 As a first step (Figure 1), an extensive literature review was conducted to develop flood vulnerability classes and associated curves based on construction types and building materials (Table 1). An increasing number of studies investigate multi-parameter damage models (e.g. Chinh et al., 2016; Wagenaar et al., 2018), but given the large amount of data required to apply such models, we here only consider studies on river floods that apply stage-damage curves. For the class and curve development, we use studies from different regions that have focused on the vulnerability of individual construction types or

10 building materials, and which are preferably based on actual event data. Some additional studies, often more qualitative in nature, were used to further refine the flood vulnerability classifications of the different building materials and construction types (e.g. Kappes et al., 2012; Laudan et al., 2017; Neubert et al., 2008; Zhai et al., 2005). Apart from reviewing the literature, experts with a structural engineering background were consulted to confirm the coherence of the final classification and vulnerability curves.

Table 1 Overview of studies used to derive construction type and building material-based vulnerability classes and curves. The four classes are: (I) non-structured buildings created by mud, adobe or informal buildings; (II) wooden buildings; (III) unreinforced masonry/concrete buildings; and (IV) reinforced masonry/concrete and steel buildings

Vuln. class	Country	Source	Data basis	Main struct. type / bldg. material	Event / applied area
I	India	Dhillon (2008)	Field survey	Mud structs.	Birupa River basin in Orissa after the 2006 flood
I	India	Maiti (2007)	Household interviews	Mud wall bldgs.	Rural areas in Orissia after the 2003 flood
I	China	Li et al. (2016)	Interviews, questionnaires, field investigation	Wood-earth structs.	Taining county town, Fujian province
I	Malawi	Rudari et al. (2016)	To generic Malawi housing typology adjusted CAPRA	Traditional (mud walls), semi-permanent (sun-dried bricks) typologies	Based on data for Northern and Central Malawi
II	India	Dhillon (2008)	Field survey	Wooden structs.	Birupa River basin in Orissa after the 2006 flood
II	Germany	Buck (2007)	Expert seminar	Wood structs.	Bldgs. in flood prone areas of Greifswald
II	New Zealand	Reese and Ramsay (2010)	Based on intl. studies and adjusted by post-event surveys	Timber bldgs.	Hutt Valley flood risk case study using major flood events in 2004 and 2007
II	Australia	Hasanzadeh Nafari et al. (2016)	Derived data of extreme events and other models	Timber wall structs.	Oueensland 2013
II	Japan	Dutta et al. (2003)	Function derived from post flood event data	Wooden structs.	Applied to case study area in Chiba prefecture
II	Guatemala	Peters Guarín et al. (2005)	Field survey, interviews	Wood frame and board construction	Flood in Samalá River tributaries related to precipitation of hurricane Mitch 1998
II	Philippines	Sagala (2006)	Field survey, household interviews	Wood, bamboo structs.	Floods in 1995 and 2004 at Naga and Bicol River in Sabang and Igualdad Barangay, Naga City
II	Romania	Godfrey et al. (2015)	Expert weighted vuln. index and curves from other studies	Wooden bldgs.	Applied to case study in Nehoiu Valley
II	India	Dhillon (2008)	Field survey	Brick, cement structs.	Birupa River basin in Orissa after the 2006 flood
III	Australia	Hasanzadeh Nafari et al. (2016)	Derived data of extreme events and other models	Masonry bldgs.	Oueensland 2013
III	Bangladesh	Islam (1997)	Household and expert interviews	Brick bldgs.	Floods between 1988 and 1993 in urban areas
III	China	Li et al. (2016)	Interviews, questionnaires, field investigation	Brick-wood and masonry structs.	2010 flood in Taining county town, Fujian province
III	Australia	Middelmann-Fernandes (2010)	Based on quantity surveyor data	Brick-veneer structs.	Swan River system in Perth, Western Australia
III	Malawi	Rudari et al. (2016)	To generic Malawi housing typology adjusted CAPRA	Permanent (burnt bricks, concrete, stone walls) typologies	Based on data for Northern and Central Malawi
III	Philippines	Sagala (2006)	Field survey, household interviews	Concrete structs.	Floods in 1995 and 2004 at Naga and Bicol River in Sabang and Igualdad Barangay, Naga City
IV	China	Li et al. (2016)	Interviews, questionnaires, field investigation	Steel-reinforced concrete structs.	2010 flood in Taining county town, Fujian province
IV	India	Maiti (2007)	Household interviews	RCC structs.	Rural areas in Orissia after the 2003 flood
IV	Germany	Buck (2007)	Expert seminar	Reinforced masonry / concrete structs.	Bldgs. in flood prone areas of Greifswald
IV	Japan	Dutta et al. (2003)	Function derived from post flood event data	RC concrete bldgs.	Applied to case study area in Chiba prefecture

Table 1 summarises the studies used to derive construction type and building material-based vulnerability classes and curves. In all of these studies, the construction type or (dominant) building material is clearly specified, and is either the only indicator, or one of the primary indicators, for the description of the flood vulnerability. Four vulnerability classes can be identified from this literature, of which each class consists of similar construction types and building materials with

5   comparable behaviour towards flooding. The four classes are: (I) non-structured buildings built of materials such as mud and adobe or informal buildings; (II) wooden buildings; (III) unreinforced masonry/concrete buildings; and (IV) reinforced masonry/concrete and steel buildings.

From the literature described in Table 1, we identified information to develop the stage-damage curve for each of these vulnerability classes. The stage-damage curves in most of the studies are concave, increasing steeply at low water depths

10   (especially for the more vulnerable materials), and with a decreasing slope at higher water depths. This overall concave shape was differentiated into curves for each of the four vulnerability classes, shown in Figure 2, using information on threshold levels (e.g. the water depth at which most damage incurred) from the studies in Table 1. We distinguish curves that go up to 2.5m and 5m (for buildings with 1- and 2-floors) as flood levels rarely reach higher levels. Housing built through informal channels dominate in Africa (World Bank, 2015), and self-constructed buildings using inexpensive materials and

15   traditional manufacturing techniques are very common (Alagbe and Opoko, 2013; Collier and Venables, 2015). Buildings of class I and II belong to this group and are assumed to be one floor only as multiple story buildings require higher quality materials and hiring a professional construction crew. The four vulnerability classes are described below:

Class I are non-structured buildings created by mud, (non-cemented) adobe blocks and other traditional materials or informal buildings. Buildings in this class can dissolve and collapse easily when impacted by flood waters. These are the most

20   vulnerable to flooding. Literature shows that mud walls will collapse when flooded by about a meter of water (Maiti, 2007), and submersion tests illustrate that most adobe bricks completely dissolve when submerged for 24 hours (Chen, 2009). These buildings are assumed to be one floor only.

Class II consists of wood frame buildings. Theoretically, these are far less vulnerable to collapsing than class I, but if wood frames become wet, they often have to be replaced, or finishing needs to be removed for drying (and replaced afterwards). In

25   a study carried out in Germany, Buck (2007) showed that damages can be ~35%-50% higher for wood frame homes than for masonry/concrete homes. However, the value of the wooden buildings in Ethiopia is much lower and they seem to be predominantly present in rural areas with more informal, less durable building material. Therefore, we decided to let the curve progress up to damage factor 1 at 2.5 m (i.e. damage can reach full building value, unlike masonry and concrete constructions). Buildings that are based on wood construction types can account for a large proportion of overall building

30   stock in some countries (e.g. USA and Ethiopia). The quality of these constructions and the building's value can vary considerably. For large-scale assessments outside of Africa, adjustment towards a greater flood resistance is recommended.

Class III are unreinforced masonry/concrete buildings. These buildings are more vulnerable than those in class IV (reinforced masonry/concrete). This is related to the fact that unreinforced walls are less able to resist pressure of water exerted on walls. However, damage is assumed to be less than class II, as masonry and concrete are less likely to need

replacement after being flooded compared to wood. Therefore, a curve between class II and class IV was created for both one and two floors.

Class IV represents reinforced masonry/concrete and steel buildings. These buildings are basically standard in most western countries and large cities in Africa. Overall, they constitute the most resistant class to flooding. Many studies (e.g. Buck,

5 2007; Li et al., 2016; Maiti, 2007) show that vulnerability curves for these types of buildings do not go up to a damage factor of 1, as some elements do not need replacement after a flood (e.g. foundation or carrying walls). This is similar to the values from Dutta et al. (2003) and HAZUS-MH (Scawthorn et al., 2006), who show examples of curves that go up to 0.6-0.7. Therefore, it is chosen to let this curve go up to 0.65. Both masonry and concrete are put in the same class.
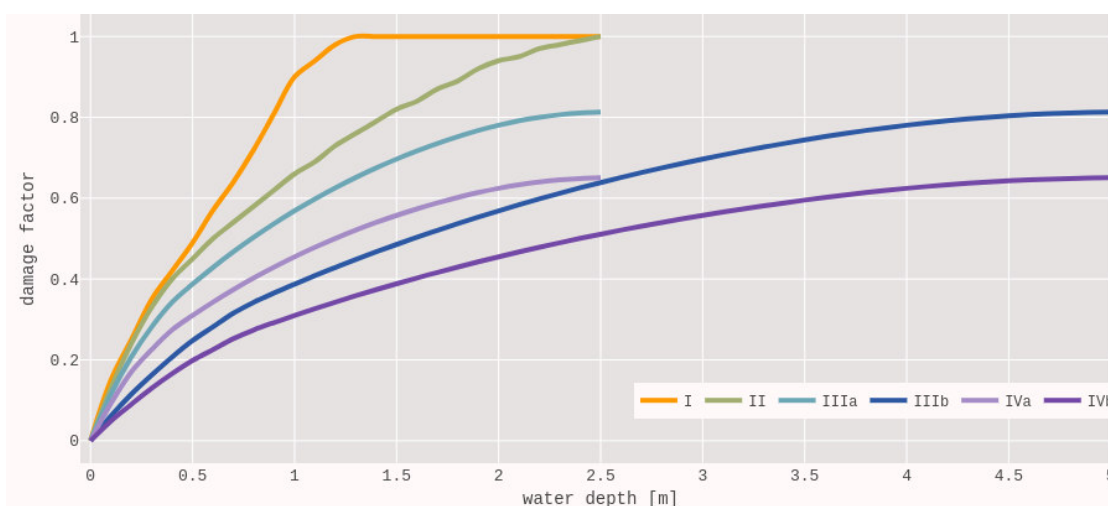
Figure 2 Stage-damage curves for four building-material-based vulnerability classes. For class III and IV the one and two floor curve are denoted by (a) and (b).

2.2. Object-based exposure data

In step 2 (Figure 1), we reclassify the objects identified in the ImageCat database into the four vulnerability classes, and

15 distinguish between urban- and rural areas. The exposure data developed by ImageCat are available on a 15" x 15" grid for several African countries. Each grid cell contains building counts for different construction types, as well as the total floor area and total building value of the cell's building stock. In total, 22 construction types are differentiated in the ImageCat data. Table 2 shows how these can be reclassified into the four vulnerability classes used in our study. In the Ethiopian data nine of these types occur.

Table 2 Construction types of the ImageCat building exposure data with their respective flood vulnerability class.

Type	Description	Vuln. class	Type	Description	Vuln. class
ADB	URM adobe bldg.	I	DS	Stone masonry bldg.	III
ERTH	Earthen bldg.	I	STN	URM stone bldg.	III
INF	Informal bldg.	I	UCB	Unreinforced concrete block bldg.	III
M	Mud walls bldg.	I	UFB	Unreinforced fired brick masonry bldg.	III
RE	Rammed earth bldg.	I	BTLR	Butler bldg. (steel frame with braced rods)	IV
WWD	Wattle & daub bldg.	I	C2	Reinforced concrete shear wall bldg.	IV
W2	Wood frame bldg.	II	C3	Non-ductile RC frame with masonry infill walls bldg.	IV
WLI	Light wood bldg.	II	MCF	Confined masonry bldg.	IV
WS	Solid wood bldg.	II	RC	Reinforced concrete frame with URM infill bldg.	IV
BRK	URM brick bldg.	III	RM	Reinforced masonry brick bldg.	IV
CB	URM concrete block bldg.	III	S	Steel bldg.	IV

Most large-scale flood assessments focus on urban areas as due to the availability of data and high potential damages. In countries with large differences between urban and rural living standards, such as developing countries, it can be expected that the share of more vulnerable buildings (i.e. class I and II) is higher in rural areas compared to urban areas (e.g. Fiadzo, 2004). To account for these differences, we classify each cell as urban or rural. If more than 50% of the ImageCat objects in a cell belong to vulnerability class I or II, the area is assumed to be predominantly rural.

To check the assumption that the share of class I and II buildings in developing countries is higher in rural areas compared to urban areas, we examined these shares in the PAGER dataset (Jaiswal and Wald, 2008). PAGER is a global building inventory at the country level, which is often used in earthquake research. PAGER provides information at a country level on the construction types that make up the total urban and rural building stock. First, we reclassified the PAGER construction types into the four flood vulnerability classes used in our study (similar to Table 2). Then, we calculated the percentage of buildings in PAGER's total urban and rural building stocks that are categorised as class I and II (Figure 3). In low and lower middle income countries, the percentage of buildings in class I and II is indeed much higher in rural areas (36%) than in urban areas (10%). The chosen threshold to identify rural areas in the ImageCat dataset (>50%) is larger than the average share we find in PAGER (Figure 3). This means that cells identified as rural using the ImageCat data information about the built environment with the chosen threshold are quite likely to indeed be rural.
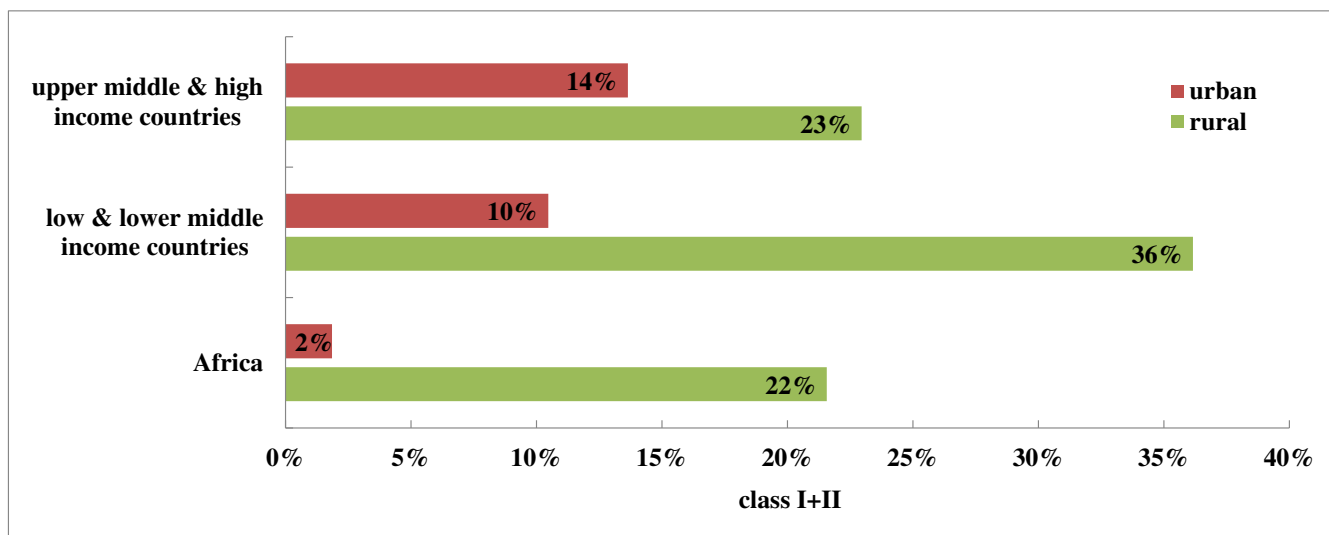
Figure 3 Average percentage of urban and rural buildings belonging to vulnerability classes I and II for different income groups and Africa according to PAGER for countries with different urban-rural inventory.

In remote sensing or land-use studies, accuracy assessments determine a process' accomplishment of classifying an image

5 (e.g. satellite data, aerial photos). Such an assessment requires reference values that represent the ground truth of the region of interest. Preferably these values are from ground collected data or hand-labelled high-resolution imagery validated by multiple interpreters (e.g. Goldblatt et al., 2018; Miyazaki et al., 2011). With these options out of the scope of this study, we examine the similarity between existing land-use products and classified areas in our approach. Compared to a strict accuracy assessment this holds the limitation of comparing already classified products. However, by benchmarking the

10 classified ImageCat data against established and recently published products, we provide an assessment of how well areas are identified in comparison. To this end, we reviewed the quality of the urban-rural ImageCat map by visual comparison with satellite imagery and by overlap with other classification products, visually and by quantifying the agreement between classified areas of the ImageCat data and other products (section 3.1). Two comparisons are made, one for urban and rural areas, and one for only urban areas. Similar to an accuracy assessment, we express the performance of this overlap by

15 calculating common comparison metrics from a confusion matrix such as overall accuracy, kappa coefficient, and producer's and user's accuracy for the sampling cells as described in Supplementary figure 1. Overall accuracy and kappa coefficient are metrics indicating the general agreement between the reference and comparison dataset. The latter two refer to the accuracy of individual classes of which the producer's accuracy describes the probability that, for example, an urban pixel is correctly classified, and the user's accuracy that a pixel classified as urban is actually urban.

20 For Ethiopia, the comparison maps are from several global land-use datasets as there are no other maps on national scale available for the country. For the reference map, the ImageCat data are assigned the reference categories 'urban', 'rural', and 'other land use' for cells outside of settlements. From the comparison maps, GHS-SMOD is the only other product that also considers rural settlements, allowing for a comparison of both urban and rural classifications. It is a relatively new product

based on the high-resolution European Joint Research Centre's Global Human Settlement layer (Pesaresi and Freire, 2016). For GHS-SMOD, built-up areas are combined with population grids to differentiate between three settlement classes: urban centres, urban clusters, and rural (Pesaresi and Freire, 2016). In order to compare to the ImageCat reference, the GHS-SMOD's urban centre and cluster cells were reassigned into a single urban class and rural cells were kept as is.

5   More products are available that provide a classification limited to urban areas, but largely overlook rural areas, such as: GRUMP (CIESIN, 2011), MOD500 (Schneider et al., 2009), the Global Urban Footprint (GUF) (Esch et al., 2017), and HBASE (Global Human Built-up And Settlement Extent) (Wang et al., 2017). GRUMP and MOD500 are widely used land cover/use datasets, with GRUMP being a 30" x 30" grid of urban extent and MOD500 based on MODIS satellite data with a 500m x 500m resolution. GUF represents built-up area based on satellite imagery with a 12m x 12m spatial resolution.

10   HBASE is a 30m x 30m Landsat derived dataset of the extent of built-up area and settlements. All these products are used in the second comparison, in which only the 'urban' classified ImageCat settlements remain in the reference map and all cells outside of these settlements are reassigned to 'other land use'. From GHS-SMOD, the urban centre and cluster cells are again combined, but rural GHS-SMOD areas are excluded in this assessment.

Both the urban-rural and the sole urban classification comparisons between the ImageCat data and the other products follow

15   a class defined stratified random sampling scheme, meaning that per class 10,000 sample points were randomly placed over the cells in each reference class. As the original maps do not all share a common geospatial model, they were reprojected to a 15" x 15" raster, using the WGS-84 datum. The results of the assessments can be found in section 3.1.

2.3. Maximum damage values

In step 3 (Figure 1), we determine the maximum damage of buildings in each vulnerability class. For a coherent set of input

20   values, we use depreciated country-specific structural maximum damage estimates per square meter as provided by the JRC report of Huizinga et al. (2017), in which residential construction costs are estimated per country using a non-linear relationship between construction costs and GDP per capita. This maximum damage value needs to be further differentiated between the four different vulnerability classes used in our study, and then multiplied by an estimate of the building footprint area per cell. This is achieved by applying the following formula for each cell:

$$D_i = \sum_1^k S \cdot N_{k,i} \cdot A_{k,i} \cdot F_k$$

25   Where

D_i is total structural maximum damage in a given cell (i), S is structural maximum damage per square metre in Ethiopia, N is the number of buildings belonging to vulnerability class k and cell i, A is the object area, meaning the building footprint for each vulnerability class k and cell i, and F is the maximum damage adjustment factor for vulnerability class k.

A and F are derived as follows:

30   *Building footprint area (A)*

As data on the footprint of different building types are not directly available, we estimated these based on floor area and number of floors derived from the ImageCat data. ImageCat provides estimates of floor areas for each construction type, based on sampling of building footprints, OSM data, interviews with local contractors and experts and literature review (Huyck and Eguchi, 2017). The country data descriptions also provide information on the typical number of floors, based on

5   sampling. For each construction type, we divided the average floor area from the ImageCat data with the number of floors, and calculated the footprint area per class (A) as the average from the construction types belonging to each class.

Our assumptions on the number of floors are derived from information in the ImageCat country data descriptions. Since buildings of construction types belonging to vulnerability class I or II rarely exceed one floor, we assumed them to have one floor in both urban and rural areas. The construction of class III and IV buildings with more than one floor requires a higher

10   skill level, mainly found in professional construction workers available in urban areas. Considering these characteristics, most class III buildings can be assumed to be one floor in rural areas. However, as most buildings in urban areas have more than one floor, we assumed class III buildings in urban areas to have two floors. Class IV buildings are assumed to be multiple floors in all areas. The resulting building footprints for Ethiopia can be found in Table 3.

15   **Table 3 Building footprints derived for Ethiopia from the ImageCat data.**

Vuln. class	Building footprint [m^2]
I	37
II	43
III 1 floor	46
III 2 floors	256
IV	467

Maximum damage adjustment factor (F)

The maximum damage values of Huizinga et al. (2017) are depreciated country-specific structural maximum damage estimates, averaged across various building types. Therefore, we differentiated these into maximum damage values for the

20   four different vulnerability classes used in our study. Huyck and Eguchi (2017) provides estimates of replacement costs for different structures, based on factors such as input material and whether the structure is owner-built or engineered using professional contractors (Huyck and Eguchi, 2017). We used these to calculate the average replacement costs for each of the four vulnerability classes, for example the average for vulnerability class I is about 95 $/sqm. In order to apply comparable maximum damage values based on a coherent dataset, these average costs per vulnerability class are then put in ratio to the

25   country-specific values from Huizinga et al. (2017), resulting in adjustment factors (F) for each vulnerability class (see Table 4) to arrive at maximum damage estimates.

Table 4 Construction cost based on Huizinga et al. (2017) and adjustment factors derived from the ImageCat data for Ethiopia.

Ethiopia construction costs	671 $
Vulnerability class	Adjustment factor
I	0.14
II	0.11
III 1 floor	0.18
III 2 floors	0.33
IV	0.48

A detailed example of the maximum damage value can be found in Supplementary figure 2. The overall Ethiopian building
5   stock is according to the ImageCat data comprised of over 16.8mln buildings. With the described approach, the total value
exposed in urban areas amounts to about $250bln compared to almost $30bln in rural areas.

2.4. Risk assessment

To calculate the damage, we combine the new exposure and vulnerability data described above, with existing hazard maps
derived from the GLOFRIS global flood risk model (WRI, 2018). These maps show inundation extent and depth at a
10   horizontal resolution of 30'' x 30'' for different return periods. The original setup of GLOFRIS is described in Ward et al.
(2013) and Winsemius et al. (2013). The maps used in this study are those developed for the current time-period in
Winsemius et al. (2015), which have been further benchmarked against observations and high-resolution local models in
Ward et al. (2017). In doing so, we estimate damage for the return periods 2, 5, 10, 25, 50, 100, 250, 500 and 1000 years.
We expressed flood risk using the commonly used metric of expected annual damage (EAD). This is estimated as the
15   integral of the flood damage curve over all exceedance probabilities (e.g. Ward et al., 2013). A source of uncertainty in flood
risk assessment is the level of incorporated flood protection. Here, we use the modelled protection standard for Ethiopia
taken from the FLOPROS database, a global database of flood protection standards developed by Scussolini et al. (2016),
namely 2 years.

3. Results and discussion

3.1. Urban-rural identification

The results of our classification of ImageCat cells for Ethiopia into urban or rural are shown in Table 5, along with summaries of data from other data sources. For rural areas, our result (7.2%) is similar to that of GHS-SMOD (6.4%), which

5 is the only other data source among the products that has a specific value for rural areas. The area in Ethiopia categorized as urban or built-up is relatively low in all data sources which is in accordance with Ethiopia being one of the least urbanized countries in Sub Saharan Africa, with the share of urban population being only between 11% and 16% (Schmidt and Kedir, 2009).

10 **Table 5 Cell areal extent of different land-use categories in Ethiopia as a percentage of the country area according to different products (original dataset projections).**

Dataset	% of country
ImageCat	urban 0.6%, rural 7.2%
GHS-SMOD	urban centre 0.4%, urban clusters 1.1%, rural 6.4%
GRUMP	urban extent 0.5%
MOD500	urban extent 0.1%
GUF	built-up area 0.1%
HBASE	built-up area and settlements 0.1%

Visual comparison

Our urban-rural classification is shown spatially in the example of Figure 4, in which we compare different land-use

15 products for an area near the City of Awasa. The urban and rural areas identified in GHS-SMOD and our classified ImageCat data show a more detailed and differentiated representation of the settlements than the coarse resolution GRUMP and MOD500 products. All products overlap in the location of main urban areas, although their extent varies. Locations of built-up areas with medium extent, for example in GUF, are hardly or not detected in HBASE, MOD500, and GRUMP, but are also seen with GHS-SMOD and our ImageCat classification.

20 Using our classification method, some smaller settlements are labelled urban with the ImageCat data, because their building stocks have high shares of class III and IV buildings, whilst GHS-SMOD classifies them as urban clusters or rural. Examples are the areas around Shashemene (see circled examples in Figure 4a). By visual inspection of Google Earth data, these seem to be areas of urban-rural transition. They have a more densely built environment than rural areas and a higher number of class III and IV buildings, which leads to the urban label in our method. Areas where cells from the ImageCat data get

25 classified as rural are also rural in GHS-SMOD or to some extent urban clusters due to a higher population density in the surrounding cells. However, the overlap of these settlements is more about the general area and less regarding a cell by cell

basis. In addition, visual inspection also showed that the small, more widespread settlements such as east of Awasa and Shashemene are correctly detected in the ImageCat data (rural areas in Figure 4a) but are not displayed in GHS-SMOD (Figure 4b). As a consequence of these issues, it can be expected that the performance of the classified ImageCat data and GHS-SMOD overlap is lower for rural than urban settlements.
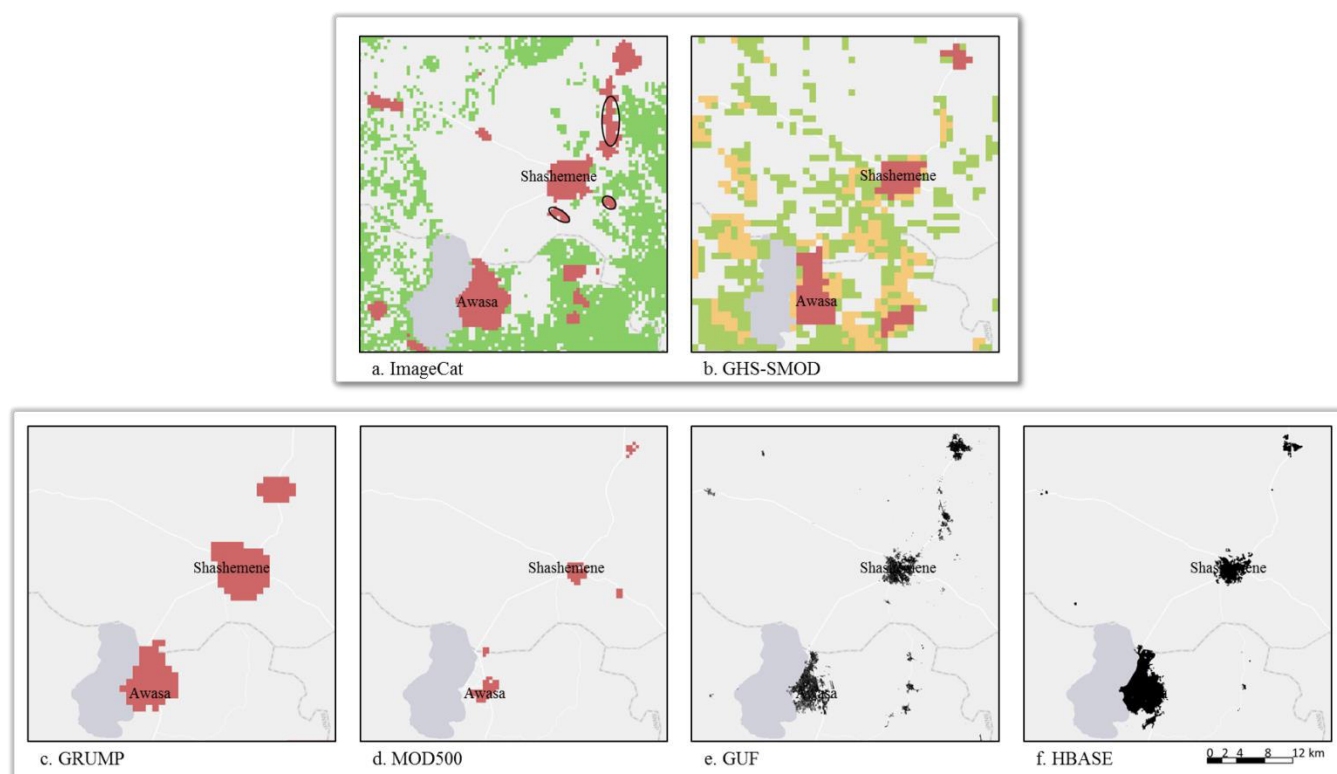
Figure 4 Illustration of urban-rural land use in the greater Awasa area in Ethiopia: (a) Urban (red) and rural (green) classified ImageCat data, (b) GHS-SMOD urban centre (red), urban cluster (yellow), rural (green), (c) GRUMP urban extent (red), (d) MOD500 urban extent (red), (e) GUF build-up area (black), (f) HBASE build-up area and settlements (black); original dataset projections.

10   *Map agreement analyses*

Map agreement has been assessed for urban-other classes, and urban-rural-other classes using confusion matrices (see Supplementary table 1 and Supplementary table 2). When comparing the urban areas (Supplementary table 3), we see that urban and built-up area cells in the GRUMP, MOD500, GUF and HBASE almost always correspond with urban cells in the ImageCat map (urban user's accuracy ~99-100%). This confirms the observations from the visual comparison (Figure 4)

15   where we see that the general location of the main urban areas are similar between the datasets. However, with the ImageCat data more medium-sized urban areas are detected which are often not in the other datasets, resulting in the low producer's accuracy (~6-26%), again confirming the visual comparison of the Awasa region.

When including rural settlements in the assessment, only GHS-SMOD and the ImageCat classification can be compared (Table 6), as they are the only datasets which distinguish rural areas. This comparison is complicated by the fact that GHS-SMOD has three categories (urban centres, urban clusters and rural). Visual comparison with satellite imagery reveals that the middle class of urban clusters are sometimes an extension of urban centres, but can also refer to higher density

5   settlements areas in rural areas. Nevertheless, for the map agreement analysis of urban-rural-other classes we grouped these urban clusters with the urban centres to form the urban class. We find that urban cells in the GHS-SMOD have a high probability to also be urban areas in the ImageCat map (urban user's accuracy of 86.3%). However, urban cells from the ImageCat data have a much lower probability to be urban in GHS-SMOD (urban producer's accuracy of 48.7%). This implies that there are various urban settlements in the ImageCat map, which are not present in in the urban group (centres

10   and clusters) of the GHS-SMOD.

The agreement of rural cells is less good as compared the urban cells, with considerably lower user's and producer's accuracies (31.3% and 11.0% respectively). Classifications of the built-up land from remote sensing based products inherently have lower accuracy levels in less developed regions and rural settings. Even high resolution products still omit large shares of built-up areas and have to improve their performance in arid regions in Africa and areas where settlements are

15   more scattered (Klotz et al., 2016; Leyk et al., 2018). We can also observe this in the visual comparison (Figure 4) where the high resolution GUF and HBASE datasets omit many of the scattered settlements that are found in the ImageCat data or GHS-SMOD. Because of these difficulties in detecting such scattered settlements, the agreement between rural areas from the ImageCat classification and in GHS-SMOD is adversely affected as one dataset might indicate rural areas that are not identified in the other.

20   Comparability of classified maps remains an issue. For example, it has been illustrated in the literature that the total urban land in global maps varies by an order of magnitude between early global earth observation products and GRUMP. Likewise, there is about a factor 5 difference between MOD500 and GRUMP (Potere et al., 2009), and the global built-up area in the high resolution GUF product is 35% less than in GHS built-up (Esch et al., 2017). ImageCat data is more specific to the African context as the other maps are based on global classification algorithms.

25   The on construction types based ImageCat classification is a distinctly different approach as compared to most classifications, which use population and/or built-up densities. This can also cause some mismatches, for instance in informal settlements in or around cities which are classified as urban when looking at densities, but would be classified as rural when looking at construction types. Our analysis showed, however, that the classification from ImageCat data is overall reasonable similar to existing datasets, includes compared to other land-use products rural settlements, and is as such a good

30   alternative for flood risk assessments as it provides the option for more detailed vulnerability curves in the analysis.

Table 6 Results of map agreement for Ethiopia using the ImageCat data classified to urban, rural, and other land use as the reference map.

Urban-Rural Map	Urban		Rural		Other land use		Overall Accuracy (%)	Kappa
	Producer's Accuracy (%)	User's Accuracy (%)	Producer's Accuracy (%)	User's Accuracy (%)	Producer's Accuracy (%)	User's Accuracy (%)		
GHS-SMOD	48.7	86.3	11.0	31.3	94.8	45.5	51.5	0.27

3.2. Flood risk assessment

Modelled flood damages for the different return periods and risk for urban and rural areas are shown in Table 7. For 2-year return periods the damages are always zero as it is assumed that these flood events would not cause overbank flooding. As can be expected, the damages in urban areas are higher, as it is a more densely concentrated built-up environment and the value of the buildings is higher. On the other hand, the majority of exposed buildings are in rural areas. To illustrate, about 88,000 buildings in urban areas are exposed to a 100-year flood event, compared to more than four times as many rural buildings.

Table 7 Simulated flood damages (in Million $ 2016) to building structures in urban and rural areas of Ethiopia, for different return periods (RP) .

	RP 2	RP 5	RP 10	RP 25	RP 50	RP 100	RP 250	RP 500	RP 1000
Rural	0	92.2	145.5	208.7	252.8	293.5	339.6	368.9	395.3
Urban	0	351.2	522.9	706.0	819.7	924.7	1,054.5	1,142.7	1,226.5

Table 8 shows the damages per return period for the different vulnerability classes. These results show that most of the damage in rural areas results from damage to buildings of class I, which are buildings with the highest vulnerability. In urban areas, the largest share of the damage results from damage to buildings of class IV; these are the buildings with the highest exposed values. In addition, this class also makes up a large share of the exposed urban buildings, about 57,000 for a 100-year flood event which is more than twice as many buildings of class III. In total more than 464,000 buildings are simulated to be affected for events with this return period, but most are in rural areas with the majority belonging to class I (58.3%) (class II 14.6%, class III 8.1%).

Table 8 Simulated flood damages (in Million $ 2016) to building structures by vulnerability class in urban and rural areas of Ethiopia, for different return periods (RP).

		RP 2	RP 5	RP 10	RP 25	RP 50	RP 100	RP 250	RP 500	RP 1000
Rural	I	0	58.9	96.6	144.2	178.2	209.6	244.9	266.9	286.5
	II	0	17.7	26.0	34.3	39.6	44.5	50.4	54.3	58.0
	III	0	15.6	22.9	30.3	35.0	39.3	44.4	47.8	50.9
	IV	0	0	0	0	0	0	0	0	0
Urban	I	0	0.6	0.9	1.3	1.6	1.9	2.2	2.4	2.5
	II	0	0.5	0.7	0.8	1.0	1.1	1.2	1.3	1.4
	III	0	62.8	93.5	126.3	146.6	165.4	188.6	204.4	219.4
	IV	0	287.3	427.7	577.5	670.5	756.3	862.5	934.6	1,003.2

The overall flood risk in Ethiopia (i.e. expected annual damage, EAD), is about $213.2mln/yr; 78% of the total EAD is in urban areas. Whilst the rural EAD is below the EAD in urban areas, it is still high in absolute terms ($46.7mln/yr). This demonstrates that neglecting damages to rural buildings in large-scale assessments may lead to a severe underestimation of total damage values. Furthermore, the flood damages in urban and rural areas have to be considered in the context of the coping capacity of the population in the respective areas. The flood vulnerability of people below the poverty line is higher, as a larger proportion of their wealth could be affected during a flood event (Winsemius et al., 2018). While this is also true for the urban poor, the livelihoods of rural people are more susceptible where services and infrastructure are limited (Komi et al., 2016).

3.3. Comparison with Aqueduct

Compared to a traditional land-use-based model, the total simulated damages in our approach are somewhat higher, but similar in magnitude. For example, the new version of the GLOFRIS model used for the Aqueduct Global Floods tool (WRI, 2018) applies the same inundation data as used in this study, but follows the common approach of using land-use-based exposure and vulnerability data, resulting in EAD for Ethiopia of $182mln/yr. The results from our approach contain much more detail on the exposed elements and their vulnerability and allow us to examine damage in urban and rural areas. Damage in urban and rural areas cannot be distinguished in GLOFRIS as it uses HYDE data (Klein Goldewijk et al., 2011) to represent exposure, which represents the urban built-up fraction per grid cell. Moreover, Figure 5 compares the land use exposure map using classified ImageCat data and HYDE for the example of Addis Ababa. As for the rest of the country, it demonstrates that datasets like the ImageCat exposure data can provide more spatial detail than the commonly used exposure maps such as HYDE used in land-use based flood risk models. Settlement extent and outlines are more distinctive, resulting in an overall better representation of affected settlement areas in the risk assessment of our approach.

Further comparison with reported losses can be found in supplementary section 1.
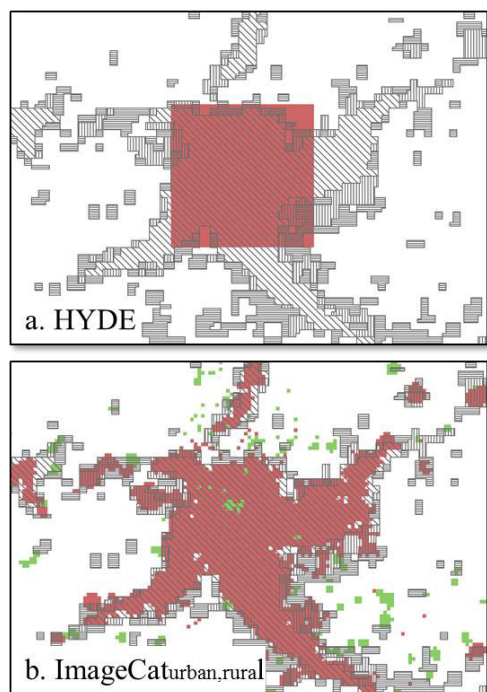
Figure 5 Addis Ababa mapped by a. HYDE as used in GLOFRIS with above 0% urban built-up (red); b. classified ImageCat data urban (red), rural (green); GHS-SMOD rural (horizontal), urban cluster (vertical), urban centre (diagonal) as background boundary reference.

3.4. Sensitivity analysis

Given the uncertainty in the input datasets and methods used in our approach, we perform a one-at-a-time sensitivity analysis to assess how the simulated EAD is affected by our assumptions on the: (a) structural maximum damage values; (b) threshold used in the urban/rural classification; (c) object area; and (d) stage-damage curves.

To assess the sensitivity of the results to the assumed values for maximum damage, we used the 90% confidence interval of estimated construction costs for residential buildings reported by Huizinga et al. (2017). These state that construction costs can be between 28% lower and 53% higher than the estimates used in this paper. For sensitivity to the threshold used in the urban/rural classification, we used thresholds of 20% and 80% for classifying urban areas, instead of the 50% used in the earlier analysis. Object areas can be very diverse between and within countries and depend on the characteristics of the housing market. For example, the Centre for affordable Housing Finance in Africa yearbooks include some indication on the average house size and price per country. However, the used sample sizes for example are very small and the average value covers only the minimum size that formal developers in urban areas are prepared to build, therefore neglecting self-built

houses. Furthermore, no differentiation between building types or constructions is given (CAHF, 2017). For the sensitivity analysis, instead of calculating the footprint areas from average floor areas across the construction types per vulnerability class, we used the most frequent floor area size per type in the ImageCat data. The building footprint sizes most affected by this are those for classes II and III (see Supplementary table 4), as the size decreased with 5 to 11m^2. The sensitivity

5   regarding the vulnerability curves is analysed by applying only one vulnerability curve, thus neglecting the differentiation our model makes toward material-based vulnerability. To this end, we selected the residential stage-damage curve used in GLOFRIS, for which the degree of damage progresses slightly below the class III one floor curve.

Table 9 Expected annual damages (in Million $ 2016 per year) compared for the normal model setup and the modified parameters
10   **used in the sensitivity analysis.**

	Normal Run	Sensitivity Analysis					
		Max. Damage		Urban-Rural		Object Area	Vuln. Curve
		lower	upper	20%	80%		
Rural	46.7	33.6	71.4	46.7	46.7	41.5	37.4
Urban	166.6	119.9	254.8	166.6	166.6	165.8	264.1
Total	213.2	153.5	326.2	213.2	213.2	207.3	301.5

Results of the sensitivity analysis are summarised in Table 9. Clearly, the flood risk estimate is very sensitive to the applied maximum damage values, as the EAD scales linearly with maximum damage changes. The results also show the EAD to be sensitive to the applied vulnerability curve. Using the single curve from GLOFRIS leads to a higher total estimate of risk by

15   41%. Therefore, the correct estimation of maximum damage values and improved representation of vulnerability are important considerations for large-scale flood risk modelling. Our approach improves the incorporation of vulnerability in the risk assessment by differentiating the built environment into classes that characterise the vulnerability of a building stock even on large scales. The EAD is very insensitive to the threshold used in the urban/rural classification. Even with the wide range of thresholds used in the sensitivity analysis, influence on the urban-rural distribution is minimal, confirming that the

20   urban and rural built environment in Ethiopia is very distinct in terms of what materials and construction types are applied. In our sensitivity analysis, the assumptions made on the object areas have little influence on the EAD, with overall slightly lower EAD when using alternative footprint sizes. Even though the effect is small here, it must be noted that these are estimated sizes and in reality building layouts are very diverse.

4. Conclusions and recommendations

In this paper, we investigated how characteristics of the built environment can be used to assess flood impacts on large scales. To this end, we developed flood vulnerability classes and curves that are based on construction types and building materials. In contrast to other large-scale flood risk models that work with aggregated land-use categories and vulnerability curves, our approach takes advantage of detailed information of the exposed elements and differentiates the vulnerabilities of these.

Showing that the predominant types of buildings are different in urban and rural areas, particularly in developing countries, the settlements' land use can be identified by the characteristics of their building stock. By distinguishing the urban and rural built environment using our vulnerability classes, we opened up the possibility to analyse flood impacts outside of the typical focus on urban areas of large-scale flood assessments. We used it to show how flood damages to buildings differ and assessed flood risk in urban and rural areas in Ethiopia. Although EAD in urban areas exceeds EAD in rural areas, the rural flood risk of \$46.7mln/yr (over 20% of total risk) is nevertheless significant. Moreover, far more buildings are affected in rural as opposed to urban areas. As low water depths can already cause major damage to the types of buildings that predominantly exist in rural settings, differentiation between flood damage in urban and rural settings could also be invaluable to studies related to poverty and flooding.

We examined the effects of parameter uncertainty and found that the model is insensitive to the applied threshold identifying urban and rural areas from the object-based information about the characteristics of building stock in the study area using our material-based vulnerability classes. Consistent with other studies (e.g. de Moel and Aerts, 2010; Merz et al., 2010), the sensitivity analysis showed that the value of the exposed buildings deserves considerable attention as we see large differences in the model output. The results further showed that aggregated vulnerability as used in large-scale land-use-based models affects the results to a great extent. In our model, vulnerability is addressed in greater detail as it reflects the behaviour of different types of buildings to floods according to their structural characteristics. Therefore, it provides a more direct relation between physical damaging processes and flood impact on different structural types.

This approach is of particular importance for studies where there is a large variation in construction types, such as large-scale studies or studies in developing countries for which the urban and rural building stock is much more differentiated. Large informal settlement areas in cities are not specifically addressed in the current setup and would be classified as rural. To acknowledge this, the urban-rural classification could be extended to highlight such areas and ones where none of the typically urban or rural building types clearly prevail. Lastly, it has to be noted that maintenance can influence the quality of the construction over the years, thus the structural vulnerability would further increase with building age.

Besides improving the accuracy in estimating direct flood losses, the use of material-based vulnerability curves also paves the road to the enhancement of multi-risk assessments as the method enables the comparison of vulnerability across different natural hazard types that also use material-based vulnerability.

Acknowledgements

This work was supported by the Netherlands Organisation for Scientific Research (NWO) in the form of VICI grant 453.140.006 for J.C.J.H.A. and VIDI grant 016.161.324 for P.J.W. The ImageCat exposure data is based on work supported by the National Aeronautics and Space Administration under Grant NNX14AQ13G, issued through the Research

5   Opportunities in Space and Earth Sciences (ROSES) Applied Sciences Program. The views and conclusions contained in this presentation are solely those of the authors.

References

Alagbe, O. A. and Opoko, A. P.: Housing Nigerian Urban Poor through Self-Build Housing Concept Using Compressed Stabilized Laterite Bricks, International Journal of Research in Social Sciences, 2, 13-18, http://eprints.covenantuniversity.edu.ng/id/eprint/3173, 2013.

5 Alfieri, L., Burek, P., Dutra, E., Krzeminski, B., Muraro, D., Thielen, J., and Pappenberger, F.: GloFAS - global ensemble streamflow forecasting and flood early warning, Hydrology and Earth System Sciences, 17, 1161-1175, doi:10.5194/hess-17-1161-2013, 2013.

Arnell, N. W. and Gosling, S. N.: The impacts of climate change on river flood risk at the global scale, Climatic Change, 134, 387-401, doi:10.1007/s10584-014-1084-5, 2016.

10 Buck, W.: Die neue DWA-Arbeitshilfe Hochwasserschadensinformationen, Fünf Jahre nach der Flut. Hochwasserschutzkonzepte - Planung, Berechnung, Realisierung. Dresdner Wasserbaukolloquium, 8. - 9. October 2007, 95-103, 2007.

CAHF: 2017 Yearbook, Housing finance in Africa, Centre for Affordable Housing Finance in Africa, Johannesburg South Africa, 8, http://housingfinanceafrica.org/app/uploads/2017_CAHF_YEARBOOK_14.10-copy.compressed.pdf, 2017.

15 Chen, G. Y. Y.: Analysis of stabilized adobe in rural East Africa, Thesis, California Polytechnic State University, San Luis Obispo, pp.99, doi:10.15368/theses.2009.149, 2009.

Chinh, D., Gain, A., Dung, N., Haase, D., and Kreibich, H.: Multi-Variate Analyses of Flood Loss in Can Tho City, Mekong Delta, Water, 8, 6, doi:10.3390/w8010006, 2016.

CIESIN: Global Rural-Urban Mapping Project, Version 1 (GRUMPv1), Urban Extents Grid, Center for International Earth
20 Science Information Network (CIESIN) Columbia University, International Food Policy Research Institute (IFPRI), The World Bank, and Centro Internacional de Agricultura Tropical (CIAT), Palisades, NY, doi:10.7927/H4GH9FVG, 2011.

Collier, P. and Venables, A. J.: Housing and Urbanization in Africa: Unleashing a Formal Market Process. In: The urban imperative: Towards competitive cities, Glaeser, E. and Joshi-Ghandi, A. (Eds.), Oxford University Press, Oxford, 413-436, 2015.

25 de Moel, H. and Aerts, J. C. J. H.: Effect of uncertainty in land use, damage models and inundation depth on flood damage estimates, Natural Hazards, 58, 407-425, doi:10.1007/s11069-010-9675-6, 2010.

de Moel, H., Jongman, B., Kreibich, H., Merz, B., Penning-Rowsell, E., and Ward, P. J.: Flood risk assessments at different spatial scales, Mitigation and Adaptation Strategies for Global Change, 20, 865-890, doi:10.1007/s11027-015-9654-z, 2015.

de Ruiter, M. C., Ward, P. J., Daniell, J. E., and Aerts, J. C. J. H.: Review Article: A comparison of flood and earthquake
30 vulnerability assessment indicators, Natural Hazards and Earth System Sciences, 17, 1231-1251, doi:10.5194/nhess-17-1231-2017, 2017.

de Villiers, G., Viljoen, G., and Booysen, H.: Standaard residensiële vloedskadefunksies vir Suid-Afrikaanse toestande (Standard residential flood damage functions for South African conditions), Suid-Afrikaanse Tydskrif vir Natuurwetenskap en Tegnologie, 26, 26-36, https://journals.co.za/content/aknat/26/1/EJC20402, 2007.

35 Dhillon, R. K.: Flood damage assessment and identification of safe routes for evacuation using a micro-level approach in part of Birupa River Basin, Orissa, India, Thesis, Indian Institute of Remote Sensing (IIRS) National Remote Sensing

Agency, International Institute for Geo-Information Science and Earth Observation (ITC) Enschede, The Netherlands, pp.145, 2008.

Dottori, F., Salamon, P., Bianchi, A., Alfieri, L., Hirpa, F. A., and Feyen, L.: Development and evaluation of a framework for global flood hazard mapping, Advances in Water Resources, 94, 87-102, doi:10.1016/j.advwatres.2016.05.002, 2016.

5   Dutta, D., Herath, S., and Musiake, K.: A mathematical model for flood loss estimation, Journal of Hydrology, 277, 24-49, doi:10.1016/S0022-1694(03)00084-2, 2003.

Esch, T., Heldens, W., Hirner, A., Keil, M., Marconcini, M., Roth, A., Zeidler, J., Dech, S., and Strano, E.: Breaking new ground in mapping human settlements from space – The Global Urban Footprint, ISPRS Journal of Photogrammetry and Remote Sensing, 134, 30-42, doi:https://doi.org/10.1016/j.isprsjprs.2017.10.012, 2017.

10 Feyen, L., Dankers, R., Bódis, K., Salamon, P., and Barredo, J. I.: Fluvial flood risk in Europe in present and future climates, Climatic Change, 112, 47-62, doi:10.1007/s10584-011-0339-7, 2011.

Fiadzo, E.: Estimating the determinants of housing quality: the case of Ghana, Joint Center for Housing Studies, Harvard University, W04-6, http://siteresources.worldbank.org/INTURBANDEVELOPMENT/Resources/336387-1268963780932/6881414-1268966662197/fiadzo.pdf, 2004.

15 Godfrey, A., Ciurean, R. L., van Westen, C. J., Kingma, N. C., and Glade, T.: Assessing vulnerability of buildings to hydro-meteorological hazards using an expert based approach – An application in Nehoiu Valley, Romania, International Journal of Disaster Risk Reduction, 13, 229-241, doi:10.1016/j.ijdrr.2015.06.001, 2015.

Goldblatt, R., Deininger, K., and Hanson, G.: Utilizing publicly available satellite data for urban research: Mapping built-up land cover and land use in Ho Chi Minh City, Vietnam, Development Engineering, 3, 83-99,
20 doi:10.1016/j.deveng.2018.03.001, 2018.

Hall, J. W., Sayers, P. B., and Dawson, R. J.: National-scale Assessment of Current and Future Flood Risk in England and Wales, Natural Hazards, 36, 147-164, doi:10.1007/s11069-004-4546-7, 2005.

Hasanzadeh Nafari, R., Ngo, T., and Lehman, W.: Calibration and validation of FLFArs - a new flood loss function for Australian residential structures, Natural Hazards and Earth System Sciences, 16, 15-27, doi:10.5194/nhess-16-15-2016,
25 2016.

Hu, Z., Huyck, C. K., Eguchi, M., and Bevington, J.: User guide: Tool for spatial inventory data development, GEM Foundation, Pavia, Italy, pp.60, doi:10.13117/GEM.DATACAPTURE.TR2014.05, 2014.

Huizinga, J., De Moel, H., and Szewczyk, W.: Global flood depth-damage functions. Methodology and the database with guidelines, European Commission Joint Research Centre, doi:10.2760/16510, 2017.

30 Huyck, C. K. and Eguchi, M.: GFDRR Africa Disaster Risk Financing - Result Area 5 Exposure Development. Replacement Cost Refinements to the Exposure data, Prepared for World Bank, GFDRR, 2017.

Ikeuchi, H., Hirabayashi, Y., Yamazaki, D., Muis, S., Ward, P. J., Winsemius, H. C., Verlaan, M., and Kanae, S.: Compound simulation of fluvial floods and storm surges in a global coupled river-coast flood model: Model development and its application to 2007 Cyclone Sidr in Bangladesh, Journal of Advances in Modeling Earth Systems, 9, 1847-1862,
35 doi:10.1002/2017ms000943, 2017.

ImageCat, CIESIN, and Porter, K.: Africa Disaster Risk Financing Phase 1 - Result Area 5, Exposure Development for 5 Sub-Saharan African countries - Ethiopia, Kenya, Uganda, Niger, Senegal, 2017.

Islam, K. M. N.: The impacts of flooding and methods of assessment in urban areas of Bangladesh, PhD thesis, Flood Hazard Research Centre, Middlesex University, pp.556, http://eprints.mdx.ac.uk/9602/, 1997.

5   Jaiswal, K. S. and Wald, D. J.: PAGER Inventory Database v2.0, U.S. Geological Survey, 2008.

Jonkman, S. N.: Advanced flood risk analysis required, Nature Clim. Change, 3, 1004-1004, doi:10.1038/nclimate2031, 2013.

Kappes, M. S., Papathoma-Köhle, M., and Keiler, M.: Assessing physical vulnerability for multi-hazards using an indicator-based methodology, Applied Geography, 32, 577-590, doi:10.1016/j.apgeog.2011.07.002, 2012.

10 Klein Goldewijk, K., Beusen, A., Van Drecht, G., and De Vos, M.: The HYDE 3.1 spatially explicit database of human-induced global land-use change over the past 12,000 years, Global Ecology and Biogeography, 20, 73-86, doi:10.1111/j.1466-8238.2010.00587.x, 2011.

Klotz, M., Kemper, T., Geiß, C., Esch, T., and Taubenböck, H.: How good is the map? A multi-scale cross-comparison framework for global settlement layers: Evidence from Central Europe, Remote Sensing of Environment, 178, 191-212, 15 doi:10.1016/j.rse.2016.03.001, 2016.

Komi, K., Amisigo, B., and Diekkrüger, B.: Integrated Flood Risk Assessment of Rural Communities in the Oti River Basin, West Africa, Hydrology, 3, 42, doi:10.3390/hydrology3040042, 2016.

Laudan, J., Rözer, V., Sieg, T., Vogel, K., and Thieken, A. H.: Damage assessment in Braunsbach 2016: data collection and analysis for an improved understanding of damaging processes during flash floods, Natural Hazards and Earth System 20 Sciences, 17, 2163-2179, doi:10.5194/nhess-17-2163-2017, 2017.

Leyk, S., Uhl, J. H., Balk, D., and Jones, B.: Assessing the Accuracy of Multi-Temporal Built-Up Land Layers across Rural-Urban Trajectories in the United States, Remote Sens Environ, 204, 898-917, doi:10.1016/j.rse.2017.08.035, 2018.

Li, W., Xu, B., and Wen, J.: Scenario-based community flood risk assessment: a case study of Taining county town, Fujian province, China, Natural Hazards, 82, 193-208, doi:10.1007/s11069-016-2187-2, 2016.

25 Maiti, S.: Defining a Flood Risk Assessment Procedure using Community Based Approach with Integration of Remote Sensing GIS. Bassed on the 2003 Orissa Flood, Thesis, Indian Institute of Remote Sensing (IIRS) National Remote Sensing Agency, International Institute for Geo-Information Science and Earth Observation (ITC) Enschede, The Netherlands, https://www.itc.nl/library/papers_2007/msc/iirs/maiti.pdf, 2007.

Mechler, R., Bouwer, L. M., Linnerooth-Bayer, J., Hochrainer-Stigler, S., Aerts, J. C. J. H., Surminski, S., and Williges, K.: 30 Managing unnatural disaster risk from climate extremes, Nature Climate Change, 4, 235-237, doi:10.1038/nclimate2137, 2014.

Merz, B., Kreibich, H., Schwarze, R., and Thieken, A.: Review article "Assessment of economic flood damage", Natural Hazards and Earth System Science, 10, 1697-1724, doi:10.5194/nhess-10-1697-2010, 2010.

Middelmann-Fernandes, M. H.: Flood damage estimation beyond stage-damage functions: an Australian example, Journal of 35 Flood Risk Management, 3, 88-96, doi:10.1111/j.1753-318X.2009.01058.x, 2010.

Miyazaki, H., Iwao, K., and Shibasaki, R.: Development of a New Ground Truth Database for Global Urban Area Mapping from a Gazetteer, Remote Sensing, 3, 1177-1187, doi:10.3390/rs3061177, 2011.

Myint, S. W., Gober, P., Brazel, A., Grossman-Clarke, S., and Weng, Q.: Per-pixel vs. object-based classification of urban land cover extraction using high spatial resolution imagery, Remote Sensing of Environment, 115, 1145-1161, doi:10.1016/j.rse.2010.12.017, 2011.

Neubert, M., Naumann, T., and Deilmann, C.: Synthetic Water Level Building Damage Relationship for GIS-supported Flood Vulnerability Modeling of Residential Properties, FLOODRISK 2008. Flood Risk Management - Research and Practice. Proceedings of the European Conference on Flood Risk Management Research into Practice, Oxford, UK 30 September - 2 October, 1717-1724, 2008.

Papathoma-Köhle, M., Gems, B., Sturm, M., and Fuchs, S.: Matrices, curves and indicators: A review of approaches to assess physical vulnerability to debris flows, Earth-Science Reviews, 171, 272-288, doi:10.1016/j.earscirev.2017.06.007, 2017.

Pesaresi, M. and Freire, S.: GHS Settlement grid following the REGIO model 2014 in application to GHSL Landsat and CIESIN GPW v4-multitemporal (1975-1990-2000-2015) European Commission Joint Research Centre (JRC), http://data.europa.eu/89h/jrc-ghsl-ghs_smod_pop_globe_r2016a, 2016.

Peters Guarín, G., van Westen, C. J., and Montoya, L.: Community-based flood risk assessment using GIS for the town of San Sebastián, Guatemala, Journal of Human Security and Development, 1, 29-49, 2005.

Potere, D., Schneider, A., Angel, S., and Civco, D. L.: Mapping urban areas on a global scale: which of the eight maps now available is more accurate?, International Journal of Remote Sensing, 30, 6531-6558, doi:10.1080/01431160903121134, 2009.

Reese, S. and Ramsay, D.: RiskScape: Flood fragility methodology, NIWA, WLG2010-45, www.victoria.ac.nz/sgees/research-centres/documents/riskscape-flood-fragility-methodology.pdf, 2010.

Rudari, R., Beckers, J., De Angeli, S., Rossi, L., and Trasforini, E.: Flood Risk Modelling for the North and Central Malawi, CIMA, ACP-EU, GFDRR, RASOR, http://www.preventionweb.net/publications/view/54387, 2016.

Sagala, S. A. H.: Analysis of flood pyhsical vulnerability in residential areas. Case Study: Naga City, the Philippines, Thesis, International Institute for Geo-Information Science and Earth Observation (ITC) Enschede, The Netherlands, 2006.

Sampson, C. C., Smith, A. M., Bates, P. D., Neal, J. C., Alfieri, L., and Freer, J. E.: A high-resolution global flood hazard model, Water Resources Research, 51, 7358-7381, doi:10.1002/2015WR016954, 2015.

Scawthorn, C., Flores, P., Blais, N., Seligson, H., Tate, E., Chang, S., Mifflin, E., Thomas, W., Murphy, J., Jones, C., and Lawrence, M.: HAZUS-MH Flood Loss Estimation Methodology. II. Damage and Loss Assessment, Natural Hazards Review, 7, 72-81, doi:doi:10.1061/(ASCE)1527-6988(2006)7:2(72), 2006.

Schmidt, E. and Kedir, M.: Urbanization and Spatial Connectivity in Ethiopia: Urban Growth Analysis Using GIS, International Food Policy Research Institute (IFPRI), Addis Ababa, Working Paper 3, www.ifpri.org/cdmref/p15738coll2/id/130941/filename/131152.pdf, 2009.

Schneider, A., Friedl, M. A., and Potere, D.: A new map of global urban extent from MODIS satellite data, Environmental Research Letters, 4, 044003, http://stacks.iop.org/1748-9326/4/i=4/a=044003, 2009.

Schwarz, J. and Maiwald, H.: Damage and loss prediction model based on the vulnerability of building types, Toronto, Canada, 6-8 May 2008 2008.

Scussolini, P., Aerts, J. C. J. H., Jongman, B., Bouwer, L. M., Winsemius, H. C., de Moel, H., and Ward, P. J.: FLOPROS: an evolving global database of flood protection standards, Natural Hazards and Earth System Sciences, 16, 1049-1061,
5 doi:10.5194/nhess-16-1049-2016, 2016.

Silva, V., Henshaw, P., Huyck, C. K., and O'Hara, M.: D5 - Final Report., GEM Foundation, Pavia, Italy, 2018.

Thieken, A. H., Olschewski, A., Kreibich, H., Kobsch, S., and Merz, B.: Development and evaluation of FLEMOps – a new Flood Loss Estimation MOdel for the private sector, WIT Press, 2008.

Trigg, M. A., Birch, C. E., Neal, J. C., Bates, P. D., Smith, A., Sampson, C. C., Yamazaki, D., Hirabayashi, Y.,
10 Pappenberger, F., Dutra, E., Ward, P. J., Winsemius, H. C., Salamon, P., Dottori, F., Rudari, R., Kappes, M. S., Simpson, A. L., Hadzilacos, G., and Fewtrell, T. J.: The credibility challenge for global fluvial flood risk analysis, Environmental Research Letters, 11, 094014, doi:10.1088/1748-9326/11/9/094014, 2016.

UNFCCC: Decision 2/CP. 19: Warsaw international mechanism for loss and damage associated with climate change impacts, FCCC/CP/2013/10/Add.1, http://unfccc.int/resource/docs/2013/cop19/eng/10a01.pdf 2013.

15 UNISDR: Sendai framework for disaster risk reduction 2015–2030, United Nations International Strategy for Disaster Reduction, Geneva, UNISDR, http://www.unisdr.org/we/inform/publications/43291, 2015.

UNSD: Demographic Yearbook 2015, UN Statistics Devision, UN Department of Economic and Social Affairs, United Nations, New York, 6, https://unstats.un.org/unsd/demographic-social/products/dyb/dybsets/2015.pdf, 2016.

UNSD: Principles and recommendations for population and housing censuses. Revision 3, UN Statistics Devision, UN
20 Department of Economic and Social Affairs, United Nations, New York, https://unstats.un.org/unsd/demographic-social/Standards-and-Methods/files/Principles_and_Recommendations/Population-and-Housing-Censuses/Series_M67rev3-E.pdf, 2017.

Wagenaar, D., Lüdtke, S., Schröter, K., Bouwer, L. M., and Kreibich, H.: Regional and Temporal Transferability of Multivariable Flood Damage Models, Water Resources Research, doi:10.1029/2017wr022233, 2018.

25 Wahab, R. and Tiong, R.: Multi-variate residential flood loss estimation model for Jakarta: an approach based on a combination of statistical techniques, Natural Hazards, 86, 779-804, doi:10.1007/s11069-016-2716-z, 2016.

Wang, P., Huang, C., Brown de Colstoun, E. C., Tilton, J. C., and Tan, B.: Global Human Built-up And Settlement Extent (HBASE) Dataset From Landsat, Palisades, NY, https://doi.org/10.7927/H4DN434S, 2017.

Ward, P. J., Jongman, B., Aerts, J. C. J. H., Bates, P. D., Botzen, W. J. W., Diaz Loaiza, A., Hallegatte, S., Kind, J. M.,
30 Kwadijk, J., Scussolini, P., and Winsemius, H. C.: A global framework for future costs and benefits of river-flood protection in urban areas, Nature Climate Change, 7, 642, doi:10.1038/nclimate3350, 2017.

Ward, P. J., Jongman, B., Salamon, P., Simpson, A., Bates, P., De Groeve, T., Muis, S., de Perez, E. C., Rudari, R., Trigg, M. A., and Winsemius, H. C.: Usefulness and limitations of global flood risk models, Nature Climate Change, 5, 712-715, doi:10.1038/nclimate2742, 2015.

Ward, P. J., Jongman, B., Weiland, F. S., Bouwman, A., van Beek, R., Bierkens, M. F. P., Ligtvoet, W., and Winsemius, H. C.: Assessing flood risk at the global scale: model setup, results, and sensitivity, Environmental Research Letters, 8, 044019, doi:10.1088/1748-9326/8/4/044019, 2013.

Winsemius, H. C., Aerts, Jeroen C. J. H., van Beek, Ludovicus P. H., Bierkens, Marc F. P., Bouwman, A., Jongman, B., Kwadijk, Jaap C. J., Ligtvoet, W., Lucas, Paul L., van Vuuren, Detlef P., and Ward, Philip J.: Global drivers of future river flood risk, Nature Climate Change, doi:10.1038/nclimate2893, 2015.

Winsemius, H. C., Jongman, B., Veldkamp, T. I. E., Hallegatte, S., Bangalore, M., and Ward, P. J.: Disaster risk, climate change, and poverty: assessing the global exposure of poor people to floods and droughts, Environment and Development Economics, 23, 328-348, doi:10.1017/s1355770x17000444, 2018.

Winsemius, H. C., Van Beek, L. P. H., Jongman, B., Ward, P. J., and Bouwman, A.: A framework for global river flood risk assessments, Hydrology and Earth System Sciences, 17, 1871-1892, doi:10.5194/hess-17-1871-2013, 2013.

World Bank: A Preliminary Assessment of Damage from the Flood and Cyclone Emergency of February-March 2000, http://siteresources.worldbank.org/INTDISMGMT/Resources/WB_flood_damages_Moz.pdf, 2000.

World Bank: Stocktaking of the Housing Sector in Sub-Saharan Africa: Challenges and Opportunities., World Bank Group, Washington, DC, https://www.openknowledge.worldbank.org/handle/10986/23358 2015.

WRI: Hotspots of global river and coastal flood risk: challenges and opportunities., World Resources Institute, Washington DC, 2018.

Wünsch, A., Herrmann, U., Kreibich, H., and Thieken, A. H.: The role of disaggregation of asset values in flood loss estimation: a comparison of different modeling approaches at the Mulde River, Germany, Environ Manage, 44, 524-541, doi:10.1007/s00267-009-9335-3, 2009.

Zhai, G., Fukuzono, T., and Ikeda, S.: Modeling Flood Damage: Case of Tokai Flood 2000, Journal of the American Water Resources Association, 41, 77-92, doi:10.1111/j.1752-1688.2005.tb03719.x, 2005.